Revising the Mechanism of the Permanganate/Oxalate Reaction

Krisztián A. Kovács,*,† Pál Gróf,‡ László Burai,§ and Miklós Riedel†

Department of Physical Chemistry, Eötvös University, H-1117 Budapest, Pázmány P. sétány 1/A, Hungary, Faculty of Medicine, Institute of Biophysics and Radiation Biology, Semmelweis University, H-1444 Budapest, Puskin u. 9, POB 263, Hungary, and Institute of Molecular and Biological Chemistry, Swiss Federal Institute of Technology Lausanne, EPFL-BCH, CH-1015 Lausanne, Switzerland

Received: July 4, 2004; In Final Form: October 3, 2004

The permanganate/oxalate reaction has been known for more than a century; however, its mechanism is still subject to debate. The latest general publication by a French group established a model that involved 14 steps including 8 equilibria. The model was found to be able to simulate experimentally observed phenomena and to account for the bistability in a continually stirred tank reactor (CSTR). However, some earlier reported observations that we found in the literature seem to be inconsistent with this model. We performed electron paramagnetic resonance (EPR) measurements and stopped-flow studies with spectrophotometrical detection to shed light on these contradictions. We found that one of the key steps of the model describing the decomposition of Mn(VII) is not acceptable at least with the indicated rate constant. The only other step in which permanganate is involved is not capable of accounting for the autocatalytic nature. Our striking observation that the reaction still can be autocatalytic when applying a large stoichiometric excess of manganous ions points out that autocatalysis cannot be purely explained by a positive Mn^{2+} feedback loop. Thus, we propose that the surface-catalyzed formation of colloidal manganese dioxide from Mn(II) and Mn(VII) provides a second positive feedback loop in the reaction.

Introduction

Though the permanganate/oxalic acid reaction and its autocatalytic nature were described almost 150 years ago,[1] its mechanism is still not elucidated. The complex and very challenging nature of its kinetics is well-illustrated by the fact that it shows bistability in a continually stirred tank reactor (CSTR),[2] and oscillatory changes in absorbance were also reported,[3] although the latter observation could not be reproduced by other authors.[4] The overall reaction can be represented by the following equation:

$$2MnO_4^- + 6H_3O^+ + 5H_2C_2O_4 = 2Mn^{2+} + 14H_2O + 10CO_2 \quad (1)$$

It can be divided into three principal sequential processes. In the first, the concentration of permanganate is relatively constant (induction period). The second is characterized by the decomposition of permanganate and the formation of at least two intermediates which are apparently Mn(IV) and Mn(III) species. The final process is slow compared to the former processes and consists of the reduction of Mn(III) to give Mn(II). Its mechanism is elucidated by the work of Taube[5] and can be summarized as follows:

$$[Mn(C_2O_4)_n]^{3-2n} \rightarrow Mn^{2+} + CO_2 + {}^{\bullet}CO_2^- + (n-1)C_2O_4^{2-} \quad (2)$$

where n can be 1, 2, or 3. The rate constants of all three first-order decompositions are known; complexes containing less oxalate decompose more rapidly. This accounts well for the observed inhibitory effects of oxalate[6] on the overall reaction because manganous ions produced in this step participate in the reduction of permanganate.

The latest proposed mechanism[7] involves 14 steps including 8 equilibria (Figure 1). It was found to simulate accurately the times of half-disappearance of permanganate and the intermediates as a function of the initial concentration of oxalic acid. The model also accounted for the experimentally observed bistability in the CSTR and reproduced the inhibitory effect of oxalic acid in a restricted concentration range.[7]

The reaction steps of this mechanism were grouped into three bulk reaction steps, giving rise to the following skeleton mechanism:

$$Mn(VII) + Mn(II) + 2e^- \xrightarrow{k_1} Mn(IV) + Mn(III) \quad (3)$$

$$Mn(IV) + e^- \xrightarrow{k_2} Mn(III) \quad (4)$$

$$Mn(III) + e^- \xrightarrow{k_3} Mn(II) \quad (5)$$

Our experiments showed that neither the reaction steps in Figure 1 nor the preceding skeleton mechanism describes the permanganate/oxalate reaction, emphasizing the need for a new, revised mechanism. Recently, we generated and analyzed several hundreds of decompositions of the overall process, containing only strictly elementary steps.[8] In this paper, we reveal our experimental data that argues against the latest published mechanism (Figure 1). Furthermore, we present evidence that the reaction still shows acceleration in the presence of excess

* Corresponding author. E-mail: Krisztian.Kovacs@iphysiol.unil.ch.
† Eötvös University.
‡ Semmelweis University.
§ Swiss Federal Institute of Technology Lausanne.

10.1021/jp047061u CCC: $27.50
Published on Web 11/20/2004

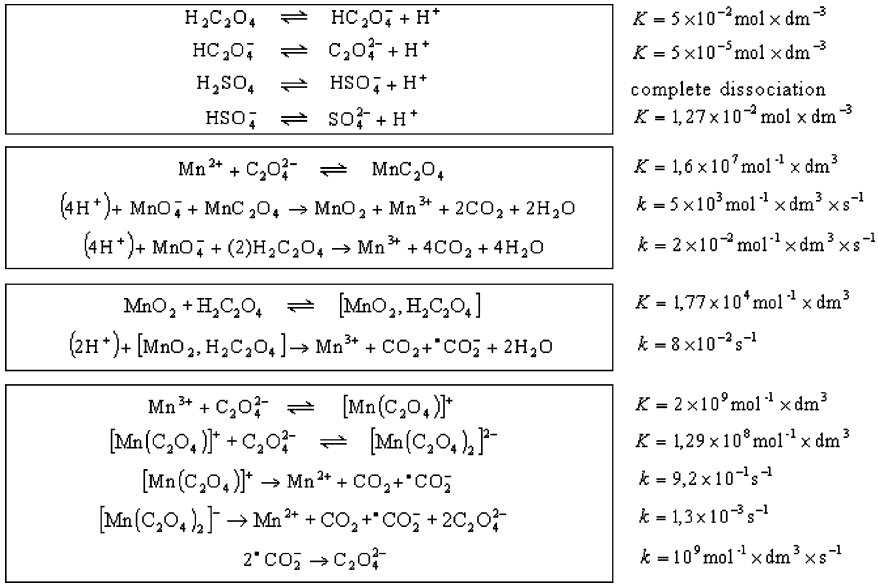

Figure 1. The proposed mechanism of the permanganate/oxalate reaction as published by Pimienta et al. in ref 7.

Mn^{2+}, pointing out the existence of a second autocatalytic species that we suppose to be colloidal MnO_2.

Experimental Section

Solutions. All solutions were prepared from commercial compounds that were dissolved in double-distilled water and used immediately. To demonstrate the blocking effect of F^- on the overall reaction, a manually mixed solution was used containing 13.77 mol/dm^3 KF, 0.004 mol/dm^3 $KMnO_4$, and 0.08 mol/dm^3 oxalic acid. Other concentration data can be found in the corresponding tables.

Matrix Rank Analysis and Rate Constant Calculation. Spectra covering the whole visual range (from 350 to 800 nm) were gathered using a Perkin-Elmer Lambda 2S spectrophotometer at 50 time points as the reaction proceeded. The resulting absorbance matrices were analyzed by the software mra306.exe[10] that can be retrieved from ftp://ftp.jate.u-szeged.hu/pub/chem/mra. The experimental uncertainty was set at 0.003 absorbance units. Concentration profiles of Mn(III), Mn(IV), and Mn(VII) for rate constant calculation were obtained by recording the changes in absorbance simultaneously at 400, 457, and 525 nm.

Electron Paramagnetic Resonance (EPR). Spectra were recorded with an X-band Bruker EMX6 on-line spectrometer equipped with a standard rectangular cavity. Modulation frequency and amplitude were 100 kHz and 2.0 G, respectively. The microwave power was set at 15 mW. Samples were measured in quartz capillaries centered in the cavity by a sample holder. The temperature of the sample was kept at 25 °C by a fine-wire thermocouple immersed into the sample and was stabilized with a precision of 0.1 °C with a closed-circuit nitrogen gas system based on Peltier-diodes.

Stopped-Flow Studies. Mn^{2+}-catalyzed reactions were measured by an SFA-20 stopped-flow device (High-Tech Scientific) coupled to an on-line SPEKTROMOM 195D spectrophotometer. Two flanking cuvettes connected to a circulating water bath kept the sample at 25 °C. Between two shots, the circuit was washed three times with oxalic acid and then five times with distilled water. Before each run, three quick shots were performed with the reactants in order to expel completely the distilled water from the cuvette. Recording started only after the third shot. Any reduction of the washing steps decreased the reproducibility of the results, presumably because of the deposition of insoluble catalytic manganese compounds in the stopped-flow circuit.

Results and Discussion

Rank Analysis of Absorbance Matrices. An obvious way to explore the kinetics of the permanganate/oxalate reaction is to record absorbance data. Earlier studies concluded the existence of three different absorbing species in the reaction.[7] A recent study applied the self-modeling curve resolution (SMCR) to determine the number of absorbing species.[9] It confirmed the number of absorbing compounds present; however, the residual spectrum did not appear completely random in the high-absorbance regions,[9] leaving a slight doubt about the occurrence of a fourth absorbing species. Thus, we decided to analyze our spectrophotometric matrices by the matrix rank analysis (MRA) method presented in ref 10. MRA was previously used in chemical analysis to determine the number of absorbing species in mixtures using spectrophotometric data without knowing the spectra of the pure components.[11] In a recent study, MRA was shown to be a valuable tool to analyze kinetic data, search for unknown absorbing intermediates, and localize their appearance in time or along the wavelength scale by calculating the residual absorbance.[10]

We performed multi-wavelength spectrophotometric measurements at 50 time points as the reaction proceeded. The absorbance matrices were analyzed by software described in ref 10.

Our results confirm that in the permanganate/oxalate reaction there are no more than three spectrophotometrically detectable intermediates (Mn(VII), Mn(IV), and Mn(III)). After subtraction of the three linearly independent spectra found by the algorithm, the residual absorbance is essentially zero along both the time and wavelength scales. An example of sequential subtractions is shown in Figure 2. First, the permanganate spectrum is subtracted and then that of the unknown Mn(IV) intermediate. The remaining absorbance can be clearly attributed to the bisoxalato−manganese(III) intermediate because a peak is evident at 457 nm. After the subtraction of this Mn(III) spectrum, the residual absorbance is close to zero, showing only random fluctuations over the whole wavelength range. Of course, this does not rule out the presence of a short-lived

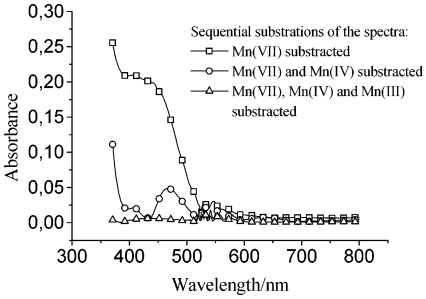

Figure 2. Calculating the residual spectra by MRA after subtracting the indicated component as described in materials and methods. Every 20th data point is depicted.

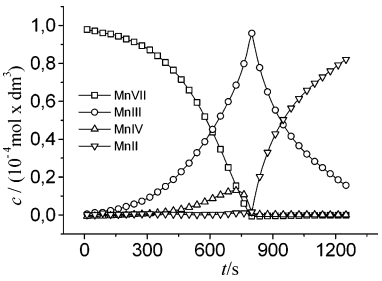

Figure 3. Concentration profiles for Mn(VII), Mn(IV), and Mn(III) derived from absorbance data using linear equations. An estimated concentration profile for Mn(II) is also depicted using the assumption formulated in ref 14. Every second data point is depicted.

absorbing intermediate (such as Mn(V) or Mn(VI)), the steady-state concentration of which would be extremely low. The irregularities that are observable on each of the three curves between 525 and 575 nm are due to the strong permanganate absorbance in that wavelength region.

Calculating Rate Constants of Some of the Reaction Steps. Because MRA has clearly demonstrated that only three species produce measurable light absorbance in the visible range, A versus t functions for each species can easily be obtained by choosing three wavelengths and resolving the following set of linear equations:

$$A_{400}(t) = A_{400}^{\mathrm{Mn(III)}}(t) + A_{400}^{\mathrm{Mn(IV)}}(t) + A_{400}^{\mathrm{Mn(VII)}}(t) \quad (6)$$

$$A_{457}(t) = A_{457}^{\mathrm{Mn(III)}}(t) + A_{457}^{\mathrm{Mn(IV)}}(t) + A_{457}^{\mathrm{Mn(VII)}}(t) \quad (7)$$

$$A_{525}(t) = A_{525}^{\mathrm{Mn(III)}}(t) + A_{525}^{\mathrm{Mn(VII)}}(t) \quad (8)$$

assuming that Mn(IV) does not absorb significant amounts of light at 525 nm. For a given species and wavelength pair, ratios of the absorbances can be calculated from the published or measured spectra. For permanganate, the following values are easily obtained from the spectrum:

$$\frac{A_{457}^{\mathrm{Mn(VII)}}(t)}{A_{400}^{\mathrm{Mn(VII)}}(t)} = 2.182 \quad (9)$$

$$\frac{A_{525}^{\mathrm{Mn(VII)}}(t)}{A_{457}^{\mathrm{Mn(VII)}}(t)} = 9.264 \quad (10)$$

For the unknown Mn(IV) intermediate, we used its published spectrum[7] and compared it to the reported[12] spectrum of colloidal MnO_2 because several authors had proposed that the unidentified Mn(IV) was manganese dioxide. Although the absorption coefficients from the two publications differed significantly, presumably reflecting the particle size of MnO_2, the following ratio was in good agreement due to the similar shape of the spectra:

$$\frac{A_{400}^{\mathrm{Mn(IV)}}(t)}{A_{457}^{\mathrm{Mn(IV)}}(t)} = 3.02 \quad (11)$$

For the bisoxalato−manganese complex, we used the published[5] spectrum. However, to confirm that it is acceptable for the in situ-generated intermediate, we took advantage of the fact that at the end of the permanganate/oxalate reaction this Mn(III) species is present for a long time as the sole absorbing compound. Thus, we simply took the ratios of the measured absorbances; the obtained values were in perfect agreement with the reported data.[6]

$$\frac{A_{457}^{\mathrm{Mn(III)}}(t)}{A_{400}^{\mathrm{Mn(III)}}(t)} = 3.29 \quad (12)$$

$$\frac{A_{457}^{\mathrm{Mn(III)}}(t)}{A_{525}^{\mathrm{Mn(III)}}(t)} = 2.38 \quad (13)$$

Using this approach, we were able to generate absorbance versus time plots for all the three species that we could convert into concentration versus time plots using the measured/published[5,7,12] absorption coefficients. We also calculated a curve for Mn(II), assuming that the vast majority of manganese is in one of the four involved oxidation states at every moment of the reaction (i.e., the following equation holds for the whole reaction time):

$$[\mathrm{Mn(II)}]_t = [\mathrm{Mn(VII)}]_0 - [\mathrm{Mn(VII)}]_t - [\mathrm{Mn(IV)}]_t - [\mathrm{Mn(III)}]_t \quad (14)$$

An example is shown in Figure 3. We were able to fit exponential functions on the first, ascending part of the Mn(IV) curves and on the second, descending part of the Mn(III) curves. The obtained k values (k_a and k_3, respectively) are presented in Table 1.

TABLE 1: Rate Constants from Spectrophotometric Studies

$[H_2C_2O_4]/[KMnO_4]$ ratio[a]	$k_3/(s^{-1})$	$k_a/(s^{-1})$
10	1.66×10^{-3}	5.66×10^{-3}
20	1.78×10^{-3}	1.37×10^{-2}
40	2.33×10^{-3}	1.94×10^{-2}
50	2.56×10^{-3}	3.02×10^{-2}

[a] Permanganate concentration was kept at 4×10^{-3} mol $\times$ dm^{-3}; oxalate concentration was varied as indicated.

Our k_3 value is in good agreement with the reported rate constants of the unimolecular decomposition of Mn(III)−oxalate complexes.[5,7] The apparent rate constant k_a cannot be assigned to a single reaction step; its importance will be discussed later.

Demonstrating the Low Steady-State Concentration of Mn^{2+} in the Initial Phase of the Reaction. Our spectrophotometric data suggest that, as long as permanganate is present in the reaction mixture, it keeps manganous concentration at a very low steady-state value by consuming manganous ions. However, only indirect evidence can be obtained on Mn^{2+} concentration by spectrophotometric measurements (cf. Figure 3). Because we intended to use the steady state as a constraint

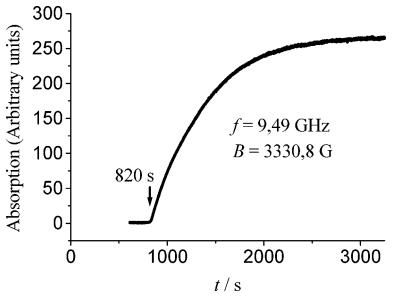

Figure 4. EPR recording at the third peak (3330.8 G) of the Mn^{2+} spectrum. No manganous ion is detectable as long as permanganate is present. (cf. with Figure 3.)

in our computations (see following text), we decided to measure the manganous concentration directly by electron spin resonance.

We performed EPR measurements at several temperatures, and the alignment of the obtained curves with the corresponding spectrophotometric data clearly shows that no manganese in the +2 oxidation state is detectable until the complete disappearance of permanganate. After that, production of Mn^{2+} occurs at the same rate as the decomposition of the bisoxalato−manganase(III) complex; an exponential function fitted on the Mn^{2+} curve gives back exactly the first-order rate constant (k_3 in Table 1) of the

$$[Mn(C_2O_4)_2]^- \rightarrow Mn^{2+} + CO_2 + {}^{\bullet}CO_2^- + 2C_2O_4^{2-} \quad (15)$$

reaction. (This step can be followed also by measuring CO_2 evolution; this approach yields exactly the same rate constant.[13]) A typical EPR curve is shown in Figure 4.

Revising the Currently Accepted Skeleton Mechanism. We found that the experimental data presented already cannot be reconciled with the skeleton mechanism (reactions 3, 4, 5) drawn up in the Introduction. The latest comprehensive study[7] that undertakes to break down the overall reaction into elementary steps uses this skeleton mechanism, the first step of which is the reduction of permanganate to Mn(III) and Mn(IV). For that step, Pimienta et al.[7] proposed the following two reactions:

$$(4H^+) + MnO_4^- + MnC_2O_4 \rightarrow MnO_2 + Mn^{3+} + 2CO_2 + 2H_2O \quad (16)$$

$$(4H^+) + MnO_4^- + 2H_2C_2O_4 \rightarrow Mn^{3+} + 4CO_2 + 4H_2O \quad (17)$$

The first reaction reflects the currently accepted theory that certain forms of Mn(II) are capable of reducing Mn(VII). However, the simulation of models (numerical integration by the semi-implicit Runge−Kutta method) containing only reaction 16 could not completely reproduce the kinetics of permanganate even after refitting all the values of the parameters (see Figure 7 in ref 7). The authors found[7] that the simplest expedient was to include reaction 17 as a second pathway for the first step of the skeleton mechanism.

The first conspicuous contradiction between reaction 17 and the literature on the permanganate/oxalate reaction is the finding that in solutions containing permanganate, oxalate, and fluoride the induction period can be lengthened almost to infinity.[14] Fluoride forms a complex with lower oxidation states of manganese, thereby inhibiting their reaction with permanganate. Oxalate alone is not able to reduce permanganate in these conditions, at least not at the rate suggested by Pimienta et al.[7] (Figure 1). We reproduced these observations first made by Launer and Yost[14] by adding a large excess of KF to the reaction mixture (see Experimental Section). The color of permanganate persisted over three days. This leads us to the conclusion that reaction 17 is not possible. After eliminating reaction 17, the remaining steps of the discussed mechanism (Figure 1) fall into three groups, each of which has a rate-determining step. Consequently, rate constants can be attributed to each step of the skeleton mechanism as follows:

$$Mn(VII) + Mn(II) + 2e^- \xrightarrow{k_1} Mn(IV) + Mn(III) \quad (18)$$

$$Mn(IV) + e^- \xrightarrow{k_2} Mn(III) \quad (19)$$

$$Mn(III) + e^- \xrightarrow{k_3} Mn(II) \quad (20)$$

Pimienta et al. showed in an experiment independent of the overall reaction that the reduction of Mn(IV) follows first-order kinetics;[6] thus, k_2 is a first-order rate constant. The Mn(III) → Mn(II) transition may occur via more parallel reaction steps because more than one kind of manganese−oxalate complex can be present at the same time in a reaction mixture. Even in that case, an apparent first-order rate constant (k_3) can be defined for the total Mn(III) reduction because the individual Mn(III) → Mn(II) steps are strictly monomolecular (reaction 5). Thus, the skeleton mechanism gives rise to the following set of differential equations:

$$\frac{d[Mn(VII)]}{dt} = -k_1[Mn(VII)][Mn(II)] \quad (21)$$

$$\frac{d[Mn(IV)]}{dt} = k_1[Mn(VII)][Mn(II)] - k_2[Mn(IV)] \quad (22)$$

$$\frac{d[Mn(III)]}{dt} = k_1[Mn(VII)][Mn(II)] + k_2[Mn(IV)] - k_3[Mn(III)] \quad (23)$$

$$\frac{d[Mn(II)]}{dt} = -k_1[Mn(VII)][Mn(II)] + k_3[Mn(III)] \quad (24)$$

Our EPR measurements (see preceding text) open up the way to reduce the number of these equations. Our experimentally determined $[Mn^{2+}]$ versus t curve demonstrates that the concentration of Mn(II) is restrained to a very low steady-state value until the complete disappearance of permanganate. Therefore, the initial phase of the reaction can be described by the following simplified set of ordinary differential equations (ODE):

$$\frac{d[Mn(VII)]}{dt} = -k_3[Mn(III)] \quad (25)$$

$$\frac{d[Mn(IV)]}{dt} = -k_2[Mn(IV)] + k_3[Mn(III)] \quad (26)$$

$$\frac{d[Mn(III)]}{dt} = k_2[Mn(IV)] \quad (27)$$

The concentration of permanganate has no influence on any of three reaction rates; thus, it is sufficient to consider only the second and third equations as a system. This reduced set of

TABLE 2: Autocatalysis Persists in the Presence of Mn^{2+} Ions

[Mn(II)]/[Mn(VII)] ratio	$[KMnO_4]$/mol/dm^3	$[MnSO_4]$/mol/dm^3	$[H_2C_2O_4]$/mol/dm^3	mean of minima of first derivatives/s	SD of minima of first derivatives/s
5	1×10^{-3}	5×10^{-3}	2.6×10^{-3}	58.1	3.2
10	1×10^{-3}	1×10^{-2}	2.6×10^{-3}	46.7	2.4
20	1×10^{-3}	2×10^{-2}	2.6×10^{-3}	25.0	1.1

ODE can then be resolved analytically, and the result is

$$[\mathrm{Mn(IV)}] = C_1 \exp(Q_1 t) + C_2 \exp(-Q_2 t) \quad (28)$$

$$[\mathrm{Mn(III)}] = C_1 R_1 \exp(Q_1 t) + C_2 R_2 \exp(-Q_2 t) \quad (29)$$

$$Q_1 = \frac{\sqrt{k_2^2 + 4k_2k_3} - k_2}{2} \quad (30)$$

$$Q_2 = \frac{k_2 + \sqrt{k_2^2 + 4k_2k_3}}{2} \quad (31)$$

$$R_1 = \frac{\sqrt{k_2^2 + 4k_2k_3} + k_2}{2k_3} \quad (32)$$

$$R_2 = \frac{k_2 - \sqrt{k_2^2 + 4k_2k_3}}{2k_3} \quad (33)$$

The second exponential expressions in each of the two eqs 28 and 29 are negligible compared to the first; thus, they can be eliminated. (At $t = 100$ s, when acceleration is scarcely visible, the first exponential expression is more than an order of magnitude greater than the second.) Consequently, the concentrations of Mn(III) and Mn(IV) are both given by an equation in which the exponent is Q_1. We determined experimentally the apparent rate constant k_a (Table 1) which would have to be identical to Q_1, and thus

$$2k_a = \frac{\sqrt{k_2^2 + 4k_2k_3} - k_2}{2} \quad (34)$$

from which we obtain that

$$k_2 = \frac{k_a^2}{k_3 - k_a} \quad (35)$$

Consequently, the difference $k_3 - k_a$ should be positive. On the basis of our spectrophotometric results, this is not the case (Table 1).

This result rules out any reaction mechanism that is based on the discussed and currently accepted skeleton mechanism consisting of reactions 3, 4, and 5. The reason for that is highlighted by the resolved ODE in the preceding paragraphs: The rate of Mn(III) reduction (k_3) that we determined experimentally is too slow to supply sufficient feedback in all the models which are based on the three bulk reaction steps (reactions 3, 4, and 5).

Experimental Proof for a Second Positive Feedback Loop in the Permanganate/Oxalate Reaction. The results discussed in the preceding paragraphs clearly show that the reduction of Mn(III) proceeds too slowly to produce sufficient Mn(II) for the observable acceleration of the overall reaction; in other words, the sudden drop in the permanganate concentration cannot be solely explained by Mn^{2+} feedback. To directly prove the existence of a second positive feedback loop in the reaction, we performed stopped-flow studies. We added a large excess of Mn(II) to the oxalic acid solution, which was then mixed in a stopped-flow device with a solution containing a stoichiometric amount of permanganate. We tested three different Mn(II)/Mn(VII) ratios, and for every ratio, we performed four independent experiments. Without any exception, we observed an acceleration on the permanganate absorption curve evidenced also by a minimum on the first derivative. (Table 2, Figures 5 and 6) These results clearly show that supplying Mn(II) in large excess is not sufficient to completely eliminate autocatalysis, although the overall reaction proceeds at a considerably faster rate at these conditions. Thus, a second positive feedback loop implying a species other than Mn^{2+} must be postulated.

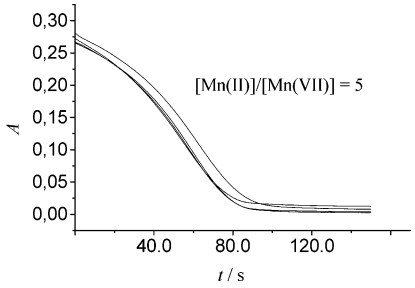

Figure 5. Acceleration in the decay of the permanganate absorbance recorded at 525 nm. Four stopped-flow runs are depicted at [Mn(II)]/[Mn(VII)] = 5. Initial concentrations are given in Table 2.

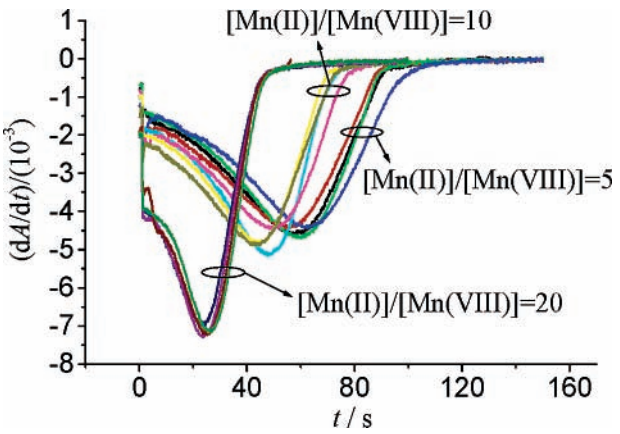

Figure 6. The first derivatives of permanganate absorption curves recorded at 525 nm. Four stopped-flow runs are depicted for each of the three [Mn(II)]/[Mn(VII)] ratios. Concentrations and minima of derivatives are given in Table 2.

Summary and Conclusions

We measured the concentration profiles of four species of the permanganate/oxalate reaction and showed that their kinetic behavior is not in agreement with the latest published mechanism.[7] Contradiction arises if the process

$$(4H^+) + MnO_4^- + MnC_2O_4 \rightarrow MnO_2 + Mn^{3+} + 2CO_2 + 2H_2O \quad (36)$$

that is currently used to explain autocatalysis is considered as a bulk reaction step in which the rate-limiting process is the collision of MnC_2O_4 and permanganate. The reason for that is the slowness of the reduction of Mn(III) into Mn(II), which does not supply enough Mn(II) to produce the observed acceleration

if it is integrated with reaction 16 in models such as Pimienta's. Thus, we conclude that step 16 is itself a complicated autocatalytic process, having its own mechanism within the whole permanganate/oxalate reaction. Using the stopped-flow technique, we demonstrated the autocatalytic nature of reaction 16, because we had observed an induction period even in the presence of a large Mn(II) excess.

We propose that the second autocatalytic agent is colloidal MnO_2 that is formed at a very high degree of dispersion and then dissolved by molecular oxalic acid. It has been known for a long time that the Guyard reaction (i.e., the synproportionation reaction between Mn(VII) and Mn(II) that yields MnO_2) is itself autocatalytic because it is catalyzed by the surface of the MnO_2 precipitate.[15] In the permanganate/oxalate reaction, the form of Mn(IV) present has been the subject of debate: Pimienta[6] concluded that it was the soluble species H_2MnO_3, but Kéki[4] reported colloidal MnO_2.

Another possible explanation for our observations would be that carboxyl radical ions could react with permanganate instead of being completely consumed by recombination. In this case, the radicals generated by the Mn(III) → Mn(II) transition would act as a second autocatalytic species by reducing permanganate ions. Light-scattering measurements may be used in the future to decide if colloidal MnO_2 is present in the reaction mixture.

Acknowledgment. We thank Gábor Peintler for help in matrix rank analysis. K.K. thanks Gábor Lente for the examples on how to use the mra306.exe software.

References and Notes

(1) Harcourt, A. V.; Esson, W. *Philos. Trans. R. Soc. (London)* **1866**, *156*, 193.
(2) Gray, P.; Scott, S. K. *Ber. Bunsen-Ges. Phys. Chem.* **1986**, *90*, 985.
(3) Fujiwara, K.; Kashima, T.; Tsubota, H.; Toyoshima, Y.; Aihara, M.; Kiboku, M. *Chem. Lett.* **1990**, *8*, 1385.
(4) Kéki, S.; Beck, M. T. *React. Kinet. Catal. Lett.* **1991**, *44*, 75.
(5) Taube, H. J. *J. Am. Chem. Soc.* **1948**, *70*, 1216.
(6) Pimienta, V.; Lavabre, D.; Levy, G.; Micheau, C. *J. Phys. Chem.* **1994**, *98*, 13294.
(7) Pimienta, V.; Lavabre, D.; Levy, G.; Micheau, C. *J. Phys. Chem.* **1995**, *99*, 14635.
(8) Kovács, K.; Vizvari, B.; Riedel, M.; Tóth, J. *Phys. Chem. Chem. Phys.* **2004**, *6*(6), 1236.
(9) Wentzell, P. D.; Wang, J. H.; Loucks, L. F.; Miller, K. M. *Can. J. Chem.* **1998**, *76*, 1144.
(10) Peintler, G.; Nagypal, I.; Jancso, A.; Epstein, I. E.; Kustin, K. *J. Phys Chem. A* **1997**, *101*, 8013.
(11) Ainsworth, S. *J. Phys. Chem.* **1961**, *65*, 1968.
(12) Baral, S.; Lume-Pereira, C.; Janata, E.; Henglein, A. *J. Phys. Chem.* **1985**, *89*, 5779.
(13) Kovács, K.; Riedel, M. *Magy. Kém. Foly.* **2000**, *106*, 405.
(14) Launer, H. F.; Yost, D. M. *J. Am. Chem. Soc.* **1934**, *56*, 2571.
(15) Polissar, M. J. *J. Phys. Chem.* **1935**, *39*, 1057.